16TH EUROPEAN CONFERENCE ON EARTHQUAKE ENGINEERING THESSALONIKI 18 - 21 JUNE 2018

FREQUENCY DEPENDENT IMPEDANCE ANALYSIS OF THE FOUNDATION-SOIL-SYSTEMS OF ONSHORE WIND TURBINES

Philipp MICHEL[1], Christoph BUTENWEG[2], Sven KLINKEL[3]

ABSTRACT

Due to the growing use of wind energy, wind turbines need to be built on sites with poor load bearing character. To increase stability und durability of the turbines, dynamic investigation of the holistic system consisting of turbine, tower and foundation, including soil-structure-interaction (SSI) effects need to be carried out. The use of different foundations, shallow or pile foundations, on varying soil conditions affects the overall dynamic behavior of the slender wind turbine tower. Therefore, a frequency tuning might be necessary while designing the tower. The influence of the SSI effects on slender structures is well known in research and practice. However, the choice of adequate and problem oriented SSI calculation belongs to the experience of the structural engineer. The available methods vary from simple analytical models to highly sophisticated numerical methods, demanding high calculation costs. This study attempts to streamline this selection process, presenting an impedance catalogue for an onshore wind turbine, to be used by practical engineers to estimate the dynamic impedance and the vibration behavior of the system in few steps. Frequency dependent impedance functions are presented for shallow and pile foundations on homogenous and layered soils. These functions are computed using the substructure method, dividing the overall system into structure and soil model. While the structure of the wind turbine is modelled via the finite element method, the soil model is constructed using the boundary element method. Concluding the holistic model is exposed to wind load to examine the SSI influence during dynamic loading.

Keywords: soil-structure-interaction, soil dynamics, vibration analysis, onshore wind turbines

1. INTRODUCTION

1.1 Motivation

Soil-structure-interaction (SSI) effects play an important role in the design of wind turbines, both offshore and onshore. The established design codes cover this field and demand SSI analyses, as the design of the wind turbine is heavily frequency dependent. In a current scientific project at RWTH Aachen University, a joint team of mechanical engineers and structural engineers from the fields of steel construction and structural dynamics investigate the overall wind turbine behaviour to improve the holistic system. Aim of the project is to minimize friction at the discipline-specific interfaces while simulating the soil-structure-drive-train interaction. In this project a reference onshore wind turbine is created which is used to carry out all simulations. This investigation focuses on the SSI part of the project.

As holistic simulations of SSI investigations are time consuming and costly, the practical engineer has to use simplifying methods. One approach is to apply the substructure method were the overall system is divided into subsystems. The current paper follows this approach, with the focus on the foundation-soil system. Impedance functions for different foundations-soil models are computed in advance and

[1]Research Assistant, Chair of Structural Analysis and Dynamics, Aachen, Germany, michel@lbb.rwth-aachen.de
[2]Professor, Center for Wind and Earthquake Engineering, Aachen, Germany, butenweg@cwe.rwth-aachen.de
[3]Professor, Chair of Structural Analysis and Dynamics, Aachen, Germany, klinkel@lbb.rwth-aachen.de

are coupled with the structure of a wind turbine in the second step. This procedure allows to carry out the complex SSI calculation in advance giving the possibility to study the SSI effects of the soil at a certain site. The wind turbine model can be modelled using highly sophisticated FE tools. Once a database of impedance functions for various soil models is created, this catalogue can be used for multiple wind turbine simulations.

1.2 State of the Art

Early SSI studies investigate vibrating machines on elastic half-space (Gazetas, 1983). Especially the response of tall and slender structures is altered by the presence of compliant soil (Luco, 1986). A milestone in analyzing the foundation-soil-behavior was the introduction of the term of the dynamic impedance function of the system (Lysmer, 1965). Kausel (2010) clearly shows the evolution of SSI computations; the next important milestone was the usage of numerical approaches, allowing the investigation of more complex systems with layered soils and deep foundations. The substructure method is a possible approach, where the structure and the soil are decoupled and determined separately. For the holistic investigation the sub-systems are coupled again. For example, the structure is modelled using the Finite Element Method (FEM) and the soil is modelled using approaches such as the Boundary Element Method (BEM). FEM-BEM coupling allows the consideration of complex soil composition as well as detailed structure modelling (Savidis et al., 2002). Taddei et al. (2014) study the SSI effects on a wind turbine based on a shallow foundation on layered soil using FEM-BEM coupling. The results are in alignment with other investigations concerning the influence of SSI on wind turbines. Bazeos et al. (2002) describe the alternation of the eigenfrequency of turbines resting on compliant soil. The findings of Zhao and Maisser (2006) confirm the influence of the SSI on the natural frequency of the turbine. Andersen (2010) applies lumped parameter models to show, that especially the higher modes of the turbine tower are damped due to the energy transmission into the ground. A simplified cone model is used by Harte et al. (2012), who show the alteration of the response in the time domain by compliant soil. The influence of layered soil on the turbine is studied in Taddei et al. (2014), which underlines the importance of the influence of the relative stiffness of structure and soil and the stiffness ratio of different soil layers. Kaynia (1982) and Garcia (2002) carry out research on the dynamic interaction of piles and soil. Pile foundations of wind turbines are in the focus of Zania (2014), who investigates the influence of the dynamic soil-pile interaction on the natural frequencies and the damping of offshore wind turbines. Present research on multi pile groups is carried out by Medina et al. (2014) who use FEM-BEM coupling to investigate the impact of pile inclination on the response of pile groups.

1.3 Goals and Outline

Impedance functions are calculated and presented for different soil models in the frequency domain using a reliable FEM-BEM code. The soil models vary from homogenous soil to multi layered soil, both shallow and pile foundations are investigated. The influence of the soil properties on the impedance functions are observed and discussed. Afterwards the impedance functions are coupled to the simplified model of a 3.2 MW onshore wind turbine model which is created in ANSYS. First it is investigated how the response of the holistic is influenced by SSI effects and how this behavior resembles the behavior of the foundation-soil substructure. Afterwards the response of the wind turbine under wind load on compliant soil is investigated in the frequency domain.

2. DYNAMIC IMPEDANCE

2.1 Soil-Structure-Interaction

The equation of motion for a structure is

$$\boldsymbol{M} \cdot \ddot{\boldsymbol{u}}(t) + \boldsymbol{C} \cdot \dot{\boldsymbol{u}}(t) + \boldsymbol{K} \cdot \boldsymbol{u}(t) = \boldsymbol{P}(t) - \boldsymbol{Q}(t) \tag{1}$$

where u is the displacement vector, and the belonging derivatives. $\boldsymbol{M}$, $\boldsymbol{C}$, und $\boldsymbol{K}$ are the mass,-displacement- and stiffness matrix. $\boldsymbol{P}$ is the load vector of the structure, while $\boldsymbol{Q}$ contains the soil reaction load. $\boldsymbol{Q}$ is used to couple the structural equation with the equation of the soil movement. The nodes in the interaction horizon are marked with the index I, while the rest carries the index R. Accordingly, the displacement and load vector yield:

$$\boldsymbol{u}(t) = \begin{Bmatrix} \boldsymbol{u}_R(t) \\ \boldsymbol{u}_I(t) \end{Bmatrix} \quad \text{and} \quad \boldsymbol{P}(t) = \begin{Bmatrix} \boldsymbol{P}_R(t) \\ \boldsymbol{P}_I(t) \end{Bmatrix} \tag{2}$$

and the overall equation of motion

$$\begin{bmatrix} \boldsymbol{M}_{RR} & \boldsymbol{M}_{RI} \\ \boldsymbol{M}_{IR} & \boldsymbol{M}_{II} \end{bmatrix} \cdot \begin{Bmatrix} \ddot{\boldsymbol{u}}_R(t) \\ \ddot{\boldsymbol{u}}_I(t) \end{Bmatrix} + \begin{bmatrix} \boldsymbol{C}_{RR} & \boldsymbol{C}_{RI} \\ \boldsymbol{C}_{IR} & \boldsymbol{C}_{II} \end{bmatrix} \cdot \begin{Bmatrix} \dot{\boldsymbol{u}}_R(t) \\ \dot{\boldsymbol{u}}_I(t) \end{Bmatrix} + \begin{bmatrix} \boldsymbol{K}_{RR} & \boldsymbol{K}_{RI} \\ \boldsymbol{K}_{IR} & \boldsymbol{K}_{II} \end{bmatrix} \cdot \begin{Bmatrix} \boldsymbol{u}_R(t) \\ \boldsymbol{u}_I(t) \end{Bmatrix} = \begin{Bmatrix} \boldsymbol{P}_R(t) \\ \boldsymbol{P}_I(t) \end{Bmatrix} - \begin{Bmatrix} \boldsymbol{0} \\ \boldsymbol{Q}(t) \end{Bmatrix} \tag{3}$$

The equation of motion can be transformed to the frequency domain via the Fast-Fourier-Transformation. Mass, stiffness and damping are introduced into the condensated dynamic stiffness matrix $\boldsymbol{K}_d$ is

$$\boldsymbol{K}_d = (\boldsymbol{K} - \boldsymbol{M}\omega^2 + i\boldsymbol{C}\omega) \tag{4}$$

Accordingly, the frequency dependent dynamic equation can be written as

$$\boldsymbol{K}_d \cdot \boldsymbol{u} = \boldsymbol{P} \tag{5}$$

In soil dynamic investigations the dynamic stiffness matrix of a system or a subsystem is called the frequency dependent impedance function, which is derived from the equation of motion, and is defined as the ratio of force and displacement

$$\boldsymbol{K}_d = (\boldsymbol{K} - \boldsymbol{M}\omega^2 + i\boldsymbol{C}\omega) = \frac{\boldsymbol{P}}{\boldsymbol{u}} \tag{6}$$

The impedance function $\boldsymbol{K}_d$ is a complex function

$$\boldsymbol{K}_d = \boldsymbol{K}_d^R + \boldsymbol{K}_d^I \tag{7}$$

The real part corresponds to the system's stiffness and mass, while the imaginary part corresponds to the damping of the system (Forchap, 1997)

$$\boldsymbol{K}^R = \boldsymbol{K} - \boldsymbol{M}\omega_p^2 \tag{8}$$

$$\boldsymbol{K}^I = i\boldsymbol{C}\omega_p \tag{9}$$

Impedance calculation can lead to negative real or dynamic parts of the dynamic stiffness. This is due to the phase shift of the vibration and not due to system instability (Studer et al., 2017)

The impedances of the foundations are calculated with the FEM-BEM code ACS SASSI. In the software the overall dynamic equation in the frequency domain yields

$$\begin{bmatrix} \boldsymbol{K}_{ii}^{III} - \boldsymbol{K}_{ii}^{II} + \boldsymbol{X}_{ii} & -\boldsymbol{K}_{iw}^{II} + \boldsymbol{X}_{iw} & \boldsymbol{K}_{is}^{III} \\ -\boldsymbol{K}_{wi}^{II} + \boldsymbol{X}_{wi} & -\boldsymbol{K}_{ww}^{II} + \boldsymbol{X}_{ww} & 0 \\ \boldsymbol{K}_{si}^{III} & 0 & \boldsymbol{K}_{ss}^{III} \end{bmatrix} \begin{Bmatrix} \boldsymbol{U}_i \\ \boldsymbol{U}_w \\ \boldsymbol{U}_s \end{Bmatrix} = \begin{Bmatrix} \boldsymbol{X}_{ii}\boldsymbol{U}_i' + \boldsymbol{X}_{iw}\boldsymbol{U}_w' \\ \boldsymbol{X}_{wi}\boldsymbol{U}_i' + \boldsymbol{X}_{ww}\boldsymbol{U}_w' \\ 0 \end{Bmatrix} \tag{10}$$

which incorporates three subsystems; the free-field site (Index *I*), the excavated soil volume for embedded foundations (*II*) and the structure itself (*III*). In this equation, $\boldsymbol{X}$ is the impedance matrix of the foundation-soil-system in the interaction nodes. $\boldsymbol{U'}$ contains the free field motion of the site.

To calculate the soil stiffness, Green's functions must be computed for the elastodynamic soil system, which is done using the Thin-Layer-Method (TLM) (Kausel, 1981). The Green's functions describe the soil flexibility, hence the relationship between a load at one point of the soil and the displacement at another point of the soil. The flexibility is the inverse of the stiffness of the soil. These fundamental solutions have to consider certain boundary conditions such as a free surface at the top and bottom boundary conditions, which are dependent on the natural soil configuration. They are able to consider a homogenous half space, a layered half space and soil layers over a bedrock. The assumption of a free surface and steadfast bedrock at the bottom provides the boundary conditions of no stress at the top and no displacements at the bottom of the model. The TLM divides the soil in multiple thin layers to calculate the relationship of a concentrated load and the displacement in one thin layer. Subsequently the stiffness matrices of each thin layer are overlapped to obtain the relationship for the complete soil model.

2.2 Validation

Before the actual investigation, the applied methods are validated. Focus is put on the impedance of the pile foundation, the systems with the higher complexity. Therefore, the dynamic impedance functions for a rectangular foundation with a 2x2 pile group are calculated and compared to results from the literature (Garcia, 2002). In this example, the rigid foundation has no contact to the soil. The ratio of the center to center distance of the piles s and the pile diameter d is $s/d = 10$, with $s = 2\ m$, and a pile diameter of 0.2 m. The foundation is resting on a homogenous soil, with an underlying homogenous half-space. Both are considered soft with an ratio of $\frac{E_{Soil}}{E_{Pile}} = 10^{-3}$ for the Young's Moduli. The soil parameters are equal for layer and half-space, additional soil and pile parameters can be found in Table 1. Figure 1 shows the real and the imaginary part of the impedance functions in vertical and horizontal direction. The complex impedance values of a pile group (index G) are normalized with the static stiffness of a single pile (index S), multiplied with the number of used piles. a_0 is the dimensionless frequency depending on the circular frequency of the harmonic vibration ω , the pile diameter d and the shear wave velocity of the soil v_s

$$a_0 = \frac{\omega\, d}{v_s} \tag{11}$$

A good agreement can be seen for the dynamic stiffness of the piles in both directions. These differences are to believed due to the employed computational methods. In general, the dynamic stiffness of the monopile shows very little frequency dependence. The present 2x2 pile group shows a strong frequency dependence in both the real and the imaginary component.

Table 1: Properties of the soil and pile model used in the validation.

System	$\boldsymbol{E}$ **[MN/m²]**	$\boldsymbol{\rho}$ **[kg/m³]**	$\boldsymbol{\mu}$ **[-]**	$\boldsymbol{v_s}$ **[m/s]**	$\boldsymbol{\beta}$ **[-]**	$\boldsymbol{L_P}$ **[m]**	$\boldsymbol{d}$ **[m]**
Soil	332.5	2000	0.40	250	0.05	-	-
Pile	332.5×10^3	2857	0.25	-	0.00	9	0.2

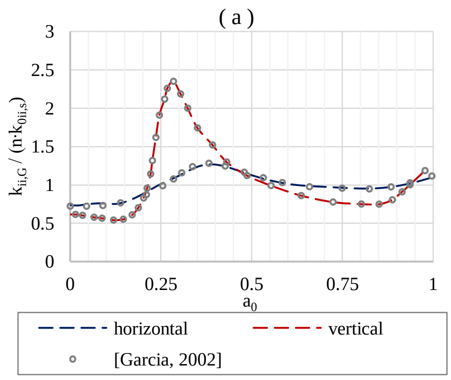

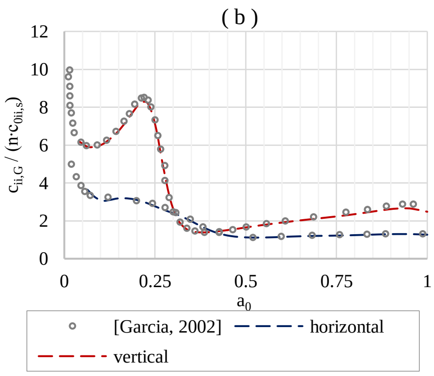

Figure 1. Dynamic impedance function in horizontal and vertical direction of a 2x2 pile group. (a) contains the real part, (b) the imaginary part.

2.3 Modelling

The model of the foundation and the pile structure are created based on the results of the pre-design of the foundations of the reference turbine. The foundation has a radius of 11 m, and is simplified to a disk with a height of 1.6 m. The pile foundation incorporates 48 piles with a length of 30 m, which are distributed periodically around the circular foundation. The piles are divided into an inner pile group inclined with 6° and an outer group inclined with 10° in the opposite direction (
Figure 2). Both foundations are described in **Σφάλμα! Το αρχείο προέλευσης της αναφοράς δεν βρέθηκε.**, which shows relevant information on the disk and the piles. The mass of the disk is 1520 tons, the overall mass of disk and all piles is 5728 tons.

Table 2: Properties of the disk and the piles of the foundations used in the dynamic investigations.

Radius [m]	**Height [m]**	**Density [t/m³]**	**Pile Diameter[m]**	**Number of piles**	**Pile length [m]**	**Damping [-]**
11	1.6	2.5	0.61	48	30	0.05

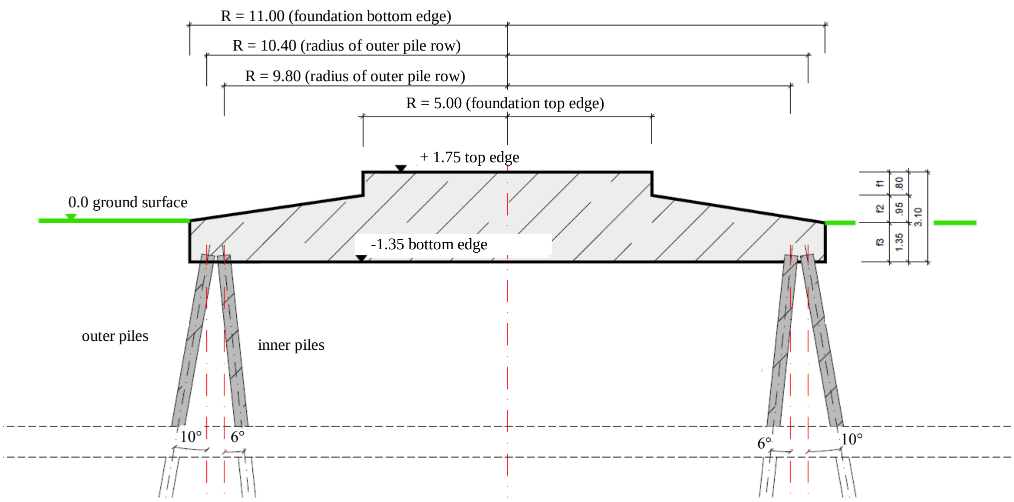

Figure 2. Geometry of the shallow and pile foundations.

While the foundation is created using solid elements, the piles are represented by beam elements. The beams are connected to the solids in multiple nodes to couple displacement and rotational degrees of freedom of the beam with the three displacement degrees of freedom of the solid element. The piles are divided in 24 parts with an element length of l_c = 1.25 m. The interaction nodes have to be located on the boundaries of the soil layers defined by the thin-layer-method. The application of the TLM (Kausel, 1981) has to follow certain conditions such as the thickness of the thin layers and the element size in the interaction horizon. The thickness of a thin layer l_c is obtained via

$$l_c = \frac{\lambda}{5} \tag{12}$$

Where the wave length λ is the ratio of the minimum shear wave velocity v_s of all the physical layers and the maximum investigated frequency f_{max}:

$$\lambda = \frac{v_s}{f_{max}} \tag{13}$$

The element size in the interaction horizon also needs to be in relation to the shear wave velocity of the top layer and the frequency to enable accurate computation. The maximum element size equals the layer thickness $l_e = \frac{\lambda}{5}$. The minimum shear wave velocity in this analysis will be 100 m/s, the maximum investigation frequency is 25 Hz. Hence the maximum soil layer thickness results to 0.8 m. The layer thickness is chosen equal to 0.625 m satisfying both conditions. The same rules apply for the element sizes in the foundation, so the maximum element edge length is 0.625 m. The mesh of the surface foundation is shown in

Figure 3. Both the surface nodes of the foundation model and the nodes of the piles are fully coupled with the soil.

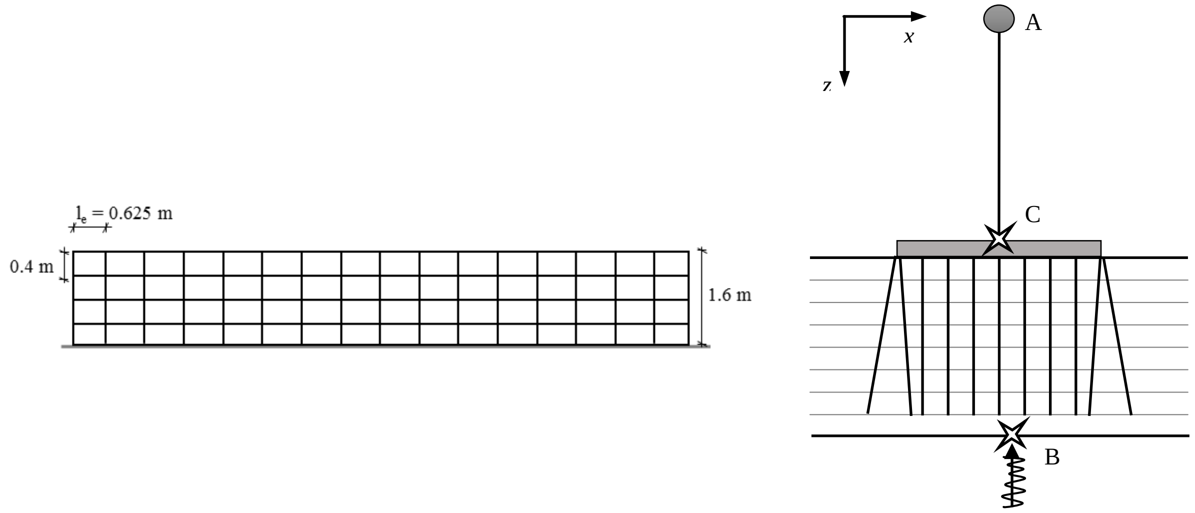

Figure 3. (left) Element size in the foundation mesh. (right) Tower model on a multi pile grid on the layered soil model The investigation point A is located at the tower top mass, point B is placed on the top of the stiff bedrock, point C at the foundation top.

2.4 Impedance Functions

The impedance functions for both foundation types are dependent on the frequency and on the soil properties like shear modulus, density and layering. Impedances for six degrees of freedom are obtained, horizontal, vertical motion, rocking and torsion in the frequency domain. With the wind turbine foundations being rotationally symmetric, the impedances in the both horizontal direction and the rocking impedances are equal.

$$
\boldsymbol{K}_{Soil}(f) = \begin{bmatrix} K_H(f) & & & & & \\ & K_H(f) & & & & \\ & & K(f)_V & & & \\ & & & K_\phi(f) & & \\ & & & & K_\phi(f) & \\ & & & & & K_T(f) \end{bmatrix} \tag{14}
$$

Figure 4 shows the horizontal impedance curves in logarithmic scale for both foundations on homogenous half spaces. The shear modulus G of the soil models ranges from 10 MN/m² to 2000 MN/m². The material damping of all soil layers is 0.05, the density is 1.9 t/m³. By applying $v_s = \sqrt{\frac{G}{\rho}}$ the corresponding shear wave velocities of the soil can be calculated. In Figure 4 (c and d) both foundation types rest on a variation of more complex soil models. A soil layer with a shear modulus of 50 MN/m² covers a homogenous half-space, bedrock and five further layered soils. The soil stiffness gradually increases with the depth.

All impedance functions are frequency dependent and contain values for the frequency domain from 0.1 Hz to 2.5 Hz with an increment of 0.1 Hz and from 2.5 Hz to 20 Hz with an increment of 0.5 Hz. While the impedances for all degrees of freedom are calculated in the interest of clarity only the horizontal direction is shown here.

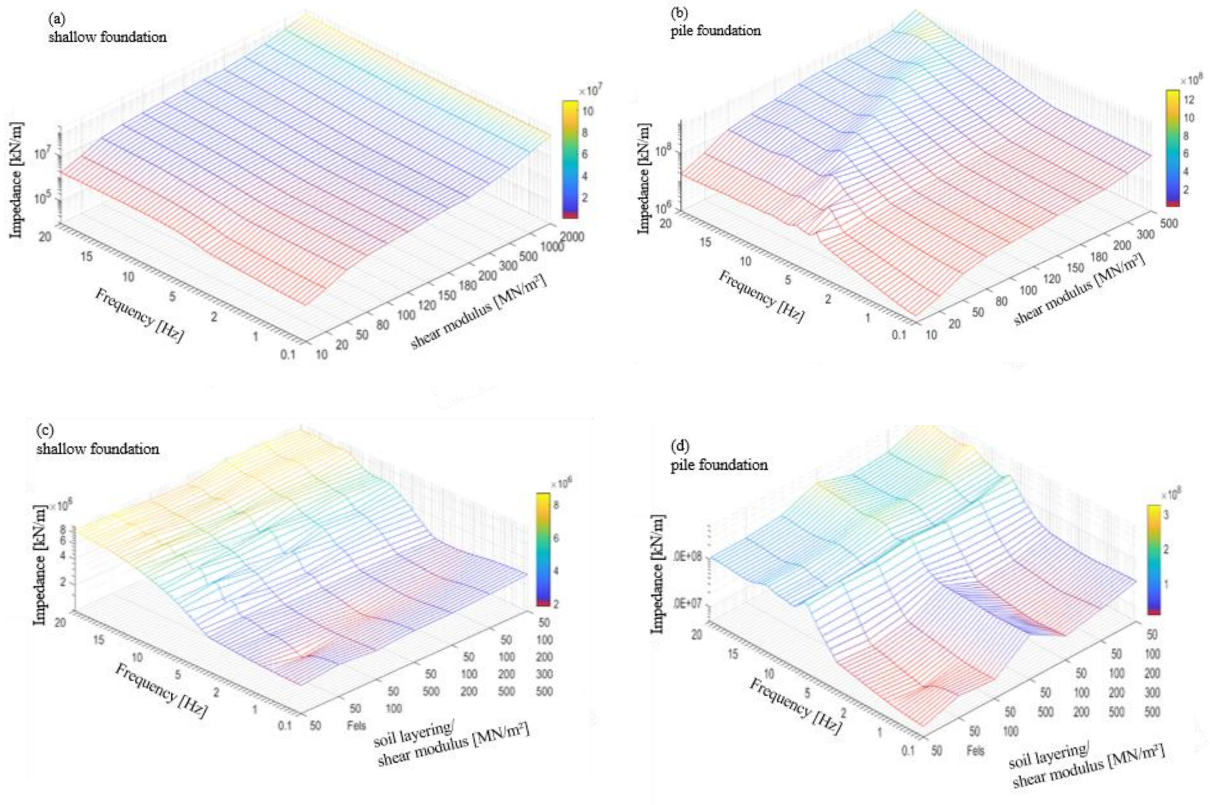

Figure 4. Horizontal impedance functions for shallow (left) or pile-grid foundations (right) on homogenous (top) and layered soil (below).

Shallow foundation on homogenous soil: The horizontal impedance of the shallow foundation on homogenous shows a steady behavior. The stiffness increases smoothly both for increasing frequencies and for stiffer soils. For 0.1 Hz the impedance of the soil with G = 500 MN/m² is 50 times higher as for the soft soil with G = 10 MN/m². The impedance of the G = 2000 MN/m² soil is 200 times higher than for the weak soil and shows rock-like behavior. This includes just a small increase of stiffness for the higher frequencies. The frequency influence is higher for the weaker soils, where the impedance curve shows a slight s-form. This includes a rise in stiffness in the range of 5 Hz. The dynamic stiffness in vertical direction is larger than in horizontal direction and the increase of stiffness is more abrupt. However, the qualitative process of the impedance is the same, which can also be said about the rocking and torsion impedance.

Pile foundation on homogenous soil: The horizontal impedance of the pile-grid on homogenous soil also increases with increasing shear modulus and increasing frequency. However, the general progress is less smooth, showing a clear eigenfrequency-peak. This peak moves in higher frequency ranges for soils with increasing stiffness. Again, a more or less abrupt rise of impedance can be seen in the 5 Hz range. This rise is most significant for soils with a medium stiffness. After the local peak, the impedances decrease again. This proofs the dynamic behavior of the system, which shows a significant eigenfrequency in this range. The qualitative progress of vertical, rocking and torsional impedance is the same. In general, the pile-grid foundation has a much larger stiffness as the shallow foundation and is more frequency dependent.

Shallow foundation on layered soil: The tendency of the increasing impedance with higher frequency and soil stiffness stays the same. However, the system shows more complex behavior with multiple local maxima and minima. The frequency increase in the 5 Hz range is more abrupt than for the homogenous half space.

Pile foundation on layered soil: The general tendency in the influence of frequency and soil stiffness stays the same. However, the curves show more maxima and minima. Significant is the maximum in the 5 Hz region for all models. The influence of the stiff section in the multi-layer soil is clearly visible, a G = 500 MN/m² soil under a softer G = 10 MN/m² layer increases the overall impedance. This effect is weaker, if multiple soft layers cover the stiff layer. In general, the complexity of the impedance curves grows for an increase in layer numbers.

The display shows the significant influence of shear modulus and frequency on the dynamic impedance of the foundation soil system. An increasing shear modulus leads to an increasing stiffness. However, the complexity of the response rises with growing system complexity in terms of soil layering and foundation type. This proves the point, that the foundation-soil-system is a dynamic system.

2.5 Impedance Catalogue

To streamline wind turbine calculations simplified models can replace the expensive numerical SSI model for certain applications. Another solution would be the development of an impedance catalogue which contains impedance functions for all degrees of freedom for different soil types. This way the engineer can choose for the suitable impedance function for the current site and couple it to the tower model.

3. HOLISTIC DYNAMIC ANALYSIS

3.1 Holistic impedance functions

To analyze the influence of the soil stiffness onto the holistic system, the impedance functions are coupled to a simplified FE model of a wind turbine tower, which is explained in
Figure 3 and Table 3. The FE structure is modelled using ANSYS.

The 3 MW reference onshore wind turbine has a hub height of 114 m. The tower of the wind turbine is presented by a beam element with a length of 112 m. The shaft and top diameter of the tower are shown in Table 3. The rotor and the engine of the wind turbine are simplified using a point mass at the tower top. The mass of flanges and connectors inside the tower are distributed equally over the tower height by increasing the density of the material to 8,5 t/m³. The Young's modulus of the steal is $2.1 \cdot 10^8 kN/m^2$, the Poisson's ratio is 0.3.

Table 3: Turbine and tower properties

Parameter	**Value**	**Parameter**	**Value**
Tower height	112 m	Min. tower diameter (top)	3.0 m
Hub height	115 m	Max. wall thickness	44 mm
Machinery mass	204 tons	Min. wall thickness	19 mm
Max. tower diameter (shaft)	5.5 m	Overall mass	595 tons

The beam element has 6 degrees of freedom for each node, the impedance functions are coupled to the bottom node. Six frequency dependent impedance functions are coupled with the beam by employing six spring-dashpot-elements (*COMBIN14*). According to the directions of motions three rotational and three translational elements are employed.
In the frequency dependent displacement computation the inverse of the dynamic stiffness $\boldsymbol{K}(f)$ of the overall system if multiplied with the load vector $\boldsymbol{P}(f)$:

$$\boldsymbol{u}(f) = \boldsymbol{K}^{-1}(f) \cdot \boldsymbol{P}(f) \tag{15}$$

The frequency dependent dynamic stiffness of the overall system consists of the condensated dynamic stiffness of the building

$$\boldsymbol{K}_{d,B}(f) = (\boldsymbol{K} - \boldsymbol{M}(2\pi f)^2 + i\boldsymbol{C} \cdot 2\pi f) \tag{16}$$

and the frequency dependent soil stiffness $\boldsymbol{K}_{Soil}(f)$ and yields

$$\boldsymbol{K}(f) = \boldsymbol{K}_{d,B} + \boldsymbol{K}_{Soil}(f) \tag{17}$$

3.2 Normalized system response

In the first step a virtual horizontal force with the amplitude of 1 is applied to the tower in each frequency. Thcorresponding horizontal displacements of the tower top and the foundation are shown in
Figure 5 for a shallow foundation and a pile foundation on soft soil and a stiff soil. While the calculation yields real and imaginary displacement parts, this investigation focuses on the amplitude of the complex displacements. The displacements are normalized by the maximum tower displacement, which occurs in the frequency range of 0.2 Hz which is the first natural frequency of the holistic tower-soil system. The corresponding eigenmode is bending of the tower, which leads to massive tower top displacements. Other eigenfrequencies can be found in higher frequency ranges where tower displacements in longitudinal direction and torsional movements occur. However, since the horizontal displacement of the tower is critical (Harte et al., 2012) the focus of this investigation lies on the first natural frequency.

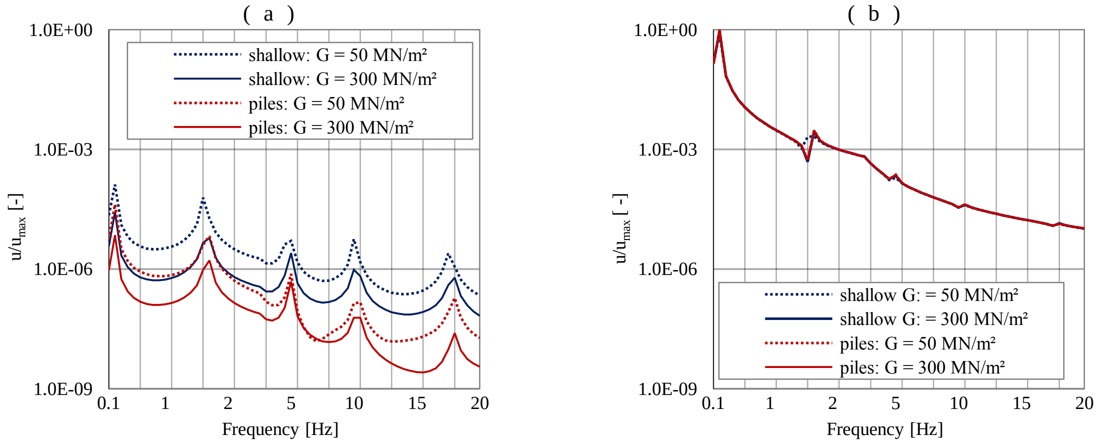

Figure 5. Normalized displacement response at the foundation top edge (left) and at the tower top (right) under a virtual load applied at the tower top node.

The normalized amplitudes at the foundation top edge (
Figure 5) show the frequency dependent influence of the SSI. The maximum displacement of all system lies in the range of the first natural frequency, the displacements are decreasing for higher frequencies. The system with soft soils yields higher response than the stiffer soils. The displacements of the shallow foundation are higher than the displacements of the pile foundation. The conclusion is, that the higher overall system stiffness leads to smaller displacement amplitudes at the foundation top edge.

The horizontal displacement at the tower top $u_{T,x}$ consists of multiple components

$$u_{T,x}(f) = u_{found,x}(f) + u_{\phi,x}(f) + u_{def,x}(f) \quad (18)$$

$u_{found,x}(f)$ Is the horizontal movement of the foundation, $u_{\phi,x}(f)$ the horizontal displacement due to rocking of the foundation and $u_{def,x}(f)$ is the displacement due to tower bending. Tower bending governs the results, as the results only vary in a small degree. However, the displacement is higher for stiff soils in certain frequency ranges. Stiff foundation boundary conditions allow no foundation movement, so the system reacts with a lot of tower bending. While only the horizontal impedance of the system is shown for brevity also the rocking impedance function obviously has an impact on the tower top motion.

3.3 Wind loading

The wind force was obtained in the joint project described in the introduction, following the current German design codes. Turbulent wind with the wind speed of 11 m/s acts on the reference turbine during energy production. The wind history is calculated for forces and moments in the three axis. The FFT is used to convert the time histories into the frequency domain. The envelope curve is used to apply the wind force in the following investigations (Werkmeister et al, 2017).

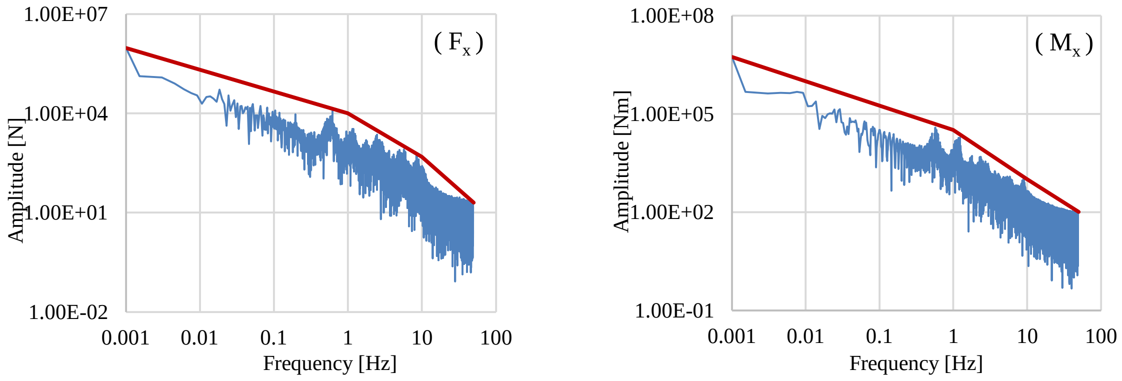

Figure 6. Envelope curve of horizontal wind force and overturning moment acting on the reference turbine.

The amplitudes of the envelope curve are shown in
Figure 6, showing the logarithmically decreasing character of the frequency dependent wind load. All wind loads act simultaneously. While only one horizontal force and one overturning moment is shown for brevity, the acting load consists of six components which are acting simultaneously. The focus of this investigation lies on the influence of the foundation-soil-impedance on the wind turbine. Because of this reason simplification of both the wind load and the tower-drive-train model seem appropriate.

The response of the turbine under wind load can be seen in
Figure 7. The response resembles the response on the virtual load in the previous chapter, soft soil lead to stronger foundation displacement. The systems enter resonance in the range of the first natural frequency (~ 0.2 Hz), which leads to an unrealistic high response. However, the response decreases logarithmically equally to the wind load. The displacements at the tower top also resemble the previous results, however, the curves vary slightly more for different soil conditions. This attests, that the frequency dependency of the holistic systems is very sensitive.

The turbine's response resembles the dynamic behavior of the impedance functions. This underlines the necessity of the dynamic analysis of the wind turbine considering SSI effects.

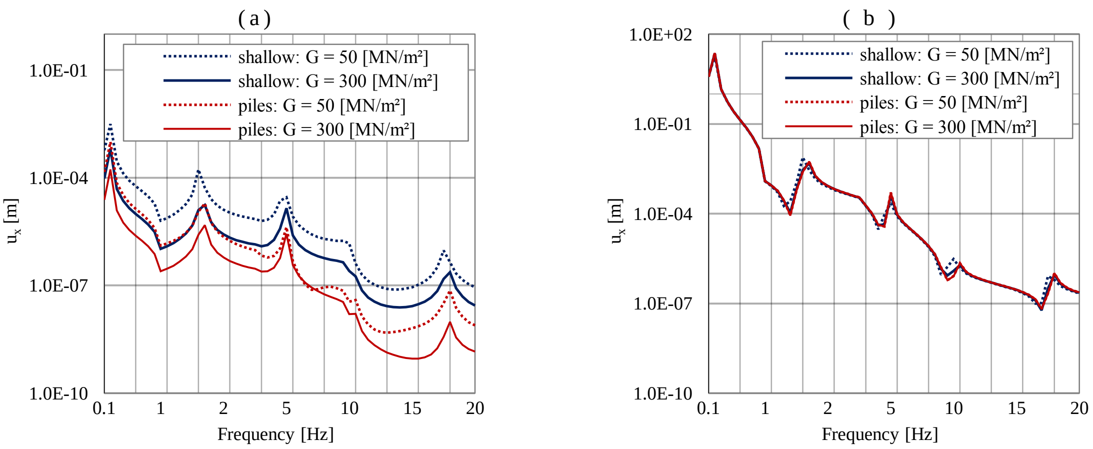

Figure 7. Horizontal displacement at the foundation top edge (left) and at the tower top (right) under a frequency dependent wind load applied at the tower top node.

4. CONCLUSIONS

The presented impedance function of shallow or pile foundations of wind turbines on compliant soil are dependent on the soil stiffness and the frequency. Strong SSI effects can be observed, especially for the more complex models, for example a multi pile foundation resting in a multi layered soil, which can be clearly seen in the frequency dependent display of the impedance functions. These impedance functions are coupled to the FE model of a wind turbine tower. The holistic system behavior resembles the influence of the SSI effects seen in the impedance functions. The application of wind load in the frequency domain shows the importance of focusing the investigations on the low frequency domain. There the wind load is highest and the natural frequencies of the holistic model are in a range of 0.2 depending on the stiffness of the soil.

While this investigation focuses on the SSI aspects, further work should focus on holistic analysis considering detailed tower and drive train modelling to simulate the overall turbine behavior.

5. ACKNOWLEDGMENTS

This research was financially supported by the German Federal Ministry for the Environment, Nature Conservation, Building and Nuclear Safety.

6. REFERENCES

Andersen, Assessment of lumped-parameter models for rigid footings, *Computers & Structures*, 88(23), pp. 1333-1347, 2010.

Bazeos, Hatzigeorgiou, Hondros, Karamaneas, Karabalis und Beskos, *Static, Seismic and stability analyses of a prototype wind turbine steel tower*, Engineering Structures, 24(8), pp. 1015-1025, 2002.

Forchap, Wellenzahlanalyse zur Ermittlung des Baugrundaufbaus bei der Untersuchung von Fundamentschwingungen und Bodenerschütterungen, *Institut für Konstruktiven Ingenieurbau Ruhr-Universität Bochum*, Bochum, 1997.

Garcia, Reduction of seismically induced structural vibrations considering soil-structure interaction, Bochum, 2002.

Gazetas, Analysis of machine foundation vibrations: state of the art, *Soil Dynamics and Earthquake Engineering*, 1983, Vol.2, No.1, 1983.

Harte, Basu, Nielsen, *Dynamic analysis of wind turbines including soil-structure-interaction*, Engineering Structures, 45, pp. 509-518, 2012.

Kausel, An Explicit Solution for the Green Functions for Dynamic Loads in Layered Media, *Massachusetts Institute of Technology*, Cambridge, 1981.

Kausel, Early history of soil-structure interaction, *Soil Dynamics and Earthquake Engineering*, pp. 822-832, September 2010.

Kaynia, Dynamic Stiffness and seismic response of pile groups, Cambridge, 1982.

Luco, Soil-structure interaction effects on the seismic response of tall chimneys, *Soil Dynamics and Earthquake Engineering*, Vol. 5, No 3, pp. 170-177, 1986.

Lysmer, Vertical Motion of Rigid Footings, *US Army Engineer Waterways Experiment Station, Corps of Engineers*, Vicksburg, 1965.

Medina, Padrón, Aznaréz, Santana, Maeso, Kinematic interaction factors of deep foundations with inclined piles, *Earthquake Engineering and Structural Dynamics* Vol. 43, pp. 2035-2050, 2014.

Savidis, Hirschauer, Bode, Schepers, 3D-simulation of dynamic interaction between track and layered subground, System Dynamics and Long-term Behaviour of Railway Vehicles, *Track and Subgrade* 6, pp. 431-450, 2002.

Studer, Laue, Koller, Bodendynamik - Grundlagen, Kennziffern, Probleme und Lösungsansätze, *Springer*, Zürich, 2007.

Taddei, Butenweg und Klinkel, Parametric Investigation of the Soil-Structure Interaction Effects on the Dynamic Behavior of a Wind Turbine Considering a Layered Soil, Hoboken: Wiley-Blackwell, 2014.

Werkmeister, Jacobs, Shkara, Michel, Fontecha (2017). Soil-Structure Drive Train Interaction of wind turbine, *World Wind Energy Conference 2017*, 12 June 2017, Malmö, Sweden.

Zania, Natural vibration frequency and damping of slender structures founded on monopiles, *Soil Dynamics and Earthquake Engineering* 59, pp. 8-20, 2014.

Zhao, Maisser, *Seismic response analysis of wind turbine towers including soil structure interaction*, Journal of Multi-Body Dynamics, 220, pp. 53-61,2006.